

Article

Straw Strip Return Increases Soil Organic Carbon Sequestration by Optimizing Organic and Humus Carbon in Aggregates of Mollisols in Northeast China

Hongli Lian ¹, Zhengyu Wang ¹, Yanan Li ¹, Haoran Xu ¹, Hongyu Zhang ², Xiangwei Gong ^{1,*}, Hua Qi ^{1,*} and Ying Jiang ¹ 

¹ Farmland Ecology Laboratory, College of Agronomy, Shenyang Agricultural University, Shenyang 110866, China; 2019200057@stu.syau.edu.cn (H.L.); 2021200073@stu.syau.edu.cn (Z.W.); lyn1020@stu.syau.edu.cn (Y.L.); xuhaoran@stu.syau.edu.cn (H.X.); jiangying@syau.edu.cn (Y.J.)

² Farming and Animal Husbandry Bureau of Tongliao, Tongliao 028005, China; zhanghongyu2006@126.com

* Correspondence: gongxiangwei@syau.edu.cn (X.G.); qihua10@syau.edu.cn (H.Q.)

Abstract: In agroecosystems, effective straw return modes are one of the key practices for increasing soil fertility and carbon (C) availability. Although they improve soil quality, there is currently little information available regarding the influence of distinct straw return modes with respect to potential soil organic carbon (SOC) sequestration. In this study, we established a five-year (2015–2019) field experiment in Mollisols of Northeast China, which included four straw return modes, plow tillage with straw return as the control (PTS), rotary tillage with straw return (RTS), rotary tillage with straw strip return (RSS), and plow tillage with straw strip return (PSS), to investigate the impact on soil physicochemical properties, aggregates, and C sequestration. The results reveal that RSS effectively improved the soil physicochemical properties. Such responses increased the contents of SOC, fulvic acid carbon (FAC), and humin carbon (HMC) in all soil layers (0–30 cm). The proportion of macroaggregates was higher in RSS, whereas the proportion of silt/clay was the lowest at depths of 0–20 cm; consequently, the mean weight diameter (MWD) and geometric mean diameter (GMD) of RSS were higher at depths of 0–20 cm due to the improved physical soil structure. In the 0–10 cm and 20–30 cm layers, the highest humic acid carbon (HAC) concentrations associated with all aggregate sizes were found for RSS, in contrast to 10–20 cm, which had increased HMC. Structural equation modeling (SEM) revealed that C transformation was mainly mediated through silt/clay-associated FAC, HMC, and SOC, ultimately determining HAC (81%) and HMC (85%) as the primary humus fractions for SOC sequestration. Therefore, this study shows that RSS is the suitable straw return mode for effectively improving soil quality, aggregate stability, and C sequestration in Mollisols of Northeast China.

Keywords: straw strip return; aggregate stability; humus; carbon sequestration



Citation: Lian, H.; Wang, Z.; Li, Y.; Xu, H.; Zhang, H.; Gong, X.; Qi, H.; Jiang, Y. Straw Strip Return Increases Soil Organic Carbon Sequestration by Optimizing Organic and Humus Carbon in Aggregates of Mollisols in Northeast China. *Agronomy* **2022**, *12*, 784. <https://doi.org/10.3390/agronomy12040784>

Academic Editor: Emanuele Lugato

Received: 8 February 2022

Accepted: 22 March 2022

Published: 24 March 2022

Publisher's Note: MDPI stays neutral with regard to jurisdictional claims in published maps and institutional affiliations.



Copyright: © 2022 by the authors. Licensee MDPI, Basel, Switzerland. This article is an open access article distributed under the terms and conditions of the Creative Commons Attribution (CC BY) license (<https://creativecommons.org/licenses/by/4.0/>).

1. Introduction

As one of the three Mollisol regions around the world, the Northeast Plain of China has a high soil organic matter content and plays a crucial role in maintaining China's agricultural productivity [1–3]. However, due to long-term agricultural intensive cultivation management (e.g., moldboard plowing) and large-scale single cropping [4,5], the soil structure and quality have been seriously degraded. Currently, the loss of soil organic carbon (SOC) content in Northeast China has exceeded 50%, even reaching 88.9% in some areas [6]. Thus, it is urgent to explore reasonable farmland management measures to improve the soil carbon (C) pool for achieving sustainable development.

Numerous studies have indicated that conservation tillage systems can effectively improve the stability of the soil structure, thereby increasing SOC sequestration and soil aggregation [7,8]. After crop straw enters the soil, straw C is first converted into labile organic

C compounds through the mineralization of microorganisms [9], and finally converted into humus C molecules through humification [10,11]. Thus, humus has different stability and turnover rates depending on its composition and can also be the most stable and recalcitrant component of the SOC pool [12,13]. Although several studies have demonstrated that crop residues regulate the compositions of soil humus [14], the stimulation effects of tillage practices with straw return on humus C fractions and on soil C sequestration lack investigation. Therefore, research on improving straw return modes is urgently needed to explore the complex relationships, and to clarify the mechanisms underlying total SOC sequestration.

Aggregates are critical indicators for evaluating soil structure and health and are also the primary sites of SOC sequestration [15,16]. The effects of different tillage and straw return modes on SOC dynamics are primarily associated with decreased soil disturbance, improved soil aggregation structure, and increased amounts of straw C input [17,18]. Around 90% of SOC is stored in soil aggregates; thereby, the size and quantity of aggregate fractions are crucial factors for evaluating the stability and C sequestration of aggregates [19]. However, conventional tillage (e.g., continuous moldboard plowing) disrupts the soil structure, decreases the stability of aggregates, and increases SOC mineralization [20]. This phenomenon generally results in the problem of C stratification, which is not favorable for C sequestration of the whole tillage layer [21]. Zhang et al. [22] reported that no-till straw return significantly increases the proportion of microaggregates (53–250 μm) and macroaggregates (>250 μm) and is associated with higher organic C concentrations in Northeast China. In contrast, although no-till straw return contributes to increasing soil surface C storage, the highest SOC sequestration is observed by rotary tillage with straw return [23], which is due to the synergistic effect of tillage and straw. Meanwhile, humus is a persistent cementing agent for C sequestration via regulation of soil aggregate formation and SOC turnover [24–26]. Recent studies have indicated that if 15% of the C from global crop residues is converted into soil humus C fractions, then global C sequestration would be approximately 5.0 Pg per year [27,28]. Thus, through tillage and straw return, understanding the mechanism of transformation between soil aggregate-associated organic C and humus C is important for improving soil C storage and soil quality.

As one of the three main grain crops in Northeast China, accounting for approximately 20% of the total national maize (*Zea mays*) area, annual maize straw production accounts for approximately 1.2×10^8 tons and 31% of the total national maize straw production [22,28,29]. To date, however, the effects of straw strip return on soil humus C and aggregate stability- and size-associated organic and humus C are still unclear. Consequently, in the present study, we hypothesize that straw strip return may have distinct effects on soil C sequestration and aggregate stability, as well as on the humus C dynamics within aggregates. The main objectives of this study were to (i) investigate the effects of straw strip return on the soil aggregate size distribution and the stability of aggregates in the cultivated layer (0–30 cm) based on five years of continuous practices; (ii) compare the responses of organic and humus C concentrations associated with bulk soil and aggregates to different straw return modes; (iii) evaluate the transformation mechanism between organic and humus C associated with bulk soil and aggregate size fractions. Our results may provide a reference for agricultural residue management in Northeast China.

2. Materials and Methods

2.1. Description of the Study Site

The long-term field experiment was established in 2015 in Tieling county, Liaoning, China (41°49' N, 124°28' E). The climate of the area is characterized by an annual average temperature of 6.8 °C and average annual precipitation of 625 mm, mainly concentrated from June to August (Figure S1). Maize (*Zea mays* L.) is the major crop cultivated in this area. The soil type is classified as Mollisol, based on descriptions by the USDA Soil Taxonomy System [30]. The initial soil conditions in the 0–30 cm layer are as follows: soil organic carbon (SOC), 11.42 g kg⁻¹; total nitrogen (TN), 0.92 g kg⁻¹; pH, 6.4; alkaline nitrogen

(AN), 132.80 mg kg⁻¹; available phosphorus (AP), 33.26 mg kg⁻¹; available potassium (AK), 161.5 mg kg⁻¹. The soil texture consisted of 16.7% sand, 58.4% silt and 24.9% clay.

2.2. Experimental Design

The long-term field experiment was arranged in a split-plot design, and the main plot factor was tillage practice (rotary and plowing tillage), whereas straw management was the subplot factor (total layer and strip straw return), with a total of four treatments and three replicate plots for each treatment, where each plot was 96 m² (9.6 m × 10 m). Four straw return modes were implemented as follows: (1) rotary tillage with straw return (RTS), using a rototiller to a depth of 15 cm (Figure 1a); (2) plow tillage with straw return (PTS) (control), a conventional tillage practice in the fields of Northeast China, using a moldboard plow to a depth of 25–30 cm (Figure 1b); (3) rotary tillage with straw strip return (RSS), in which the sowing rows were not disturbed and only the monopoly furrows were rotary tilled and combined with straw return (Figure 1c); (4) plow tillage with straw strip return (PSS), in which the sowing rows were not destroyed and only the monopoly furrows were plowed and combined with straw return (Figure 1d). The density of maize was 67,500 plants ha⁻¹. Moreover, the amount of straw returned to the field was 9000 kg ha⁻¹. Mineral NPK fertilizers (75 kg ha⁻¹ of N, 90 kg ha⁻¹ of P₂O₅, and 90 kg ha⁻¹ of K₂O) were applied annually during sowing, and 150 kg ha⁻¹ of N fertilizer was applied in the maize jointing stage. Sowing of maize in May and harvesting in October and no artificial irrigation took place during the growing season of maize.

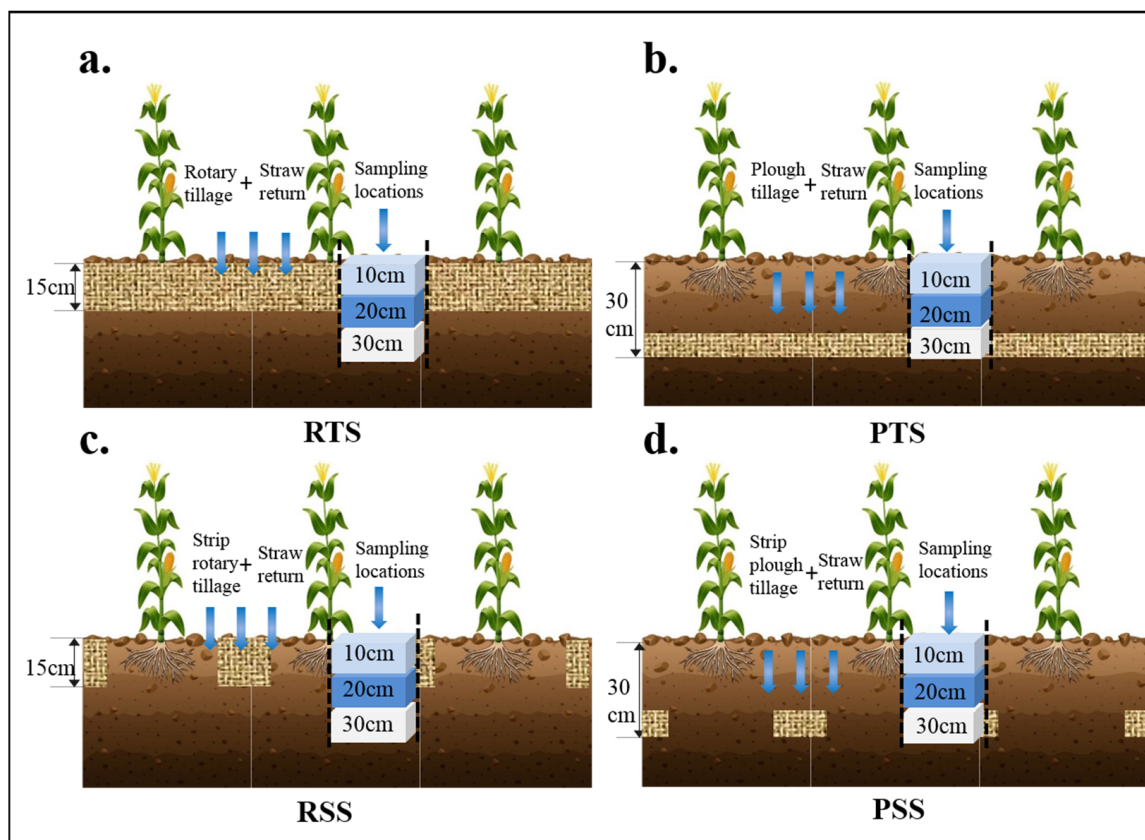


Figure 1. Diagram indicating the straw return mode of each treatment as shown in the figure. (a) RTS, rotary tillage with straw return; (b) PTS, plow tillage with straw return; (c) RSS, rotary tillage with straw strip return; (d) PSS, plow tillage with straw strip return, respectively. The tillage layer (0–30 cm) was divided into three layers, topsoil (0–10 cm), mid-soil (10–20 cm) and subsoil (20–30 cm), respectively.

2.3. Soil Sampling

Before the maize harvest in October 2019, soil samples were collected from three soil layers: 0–10, 10–20, and 20–30 cm. Additionally, in the three replicate plots, each plot was compounded into a sub-sample using the “S-shaped” sampling method, the sampling location of each plot was selected as a burrow. The collected bulk soil is placed in plastic boxes for the separation of aggregates. The rest of the soil samples were passed through a 2 mm sieve, removing vegetable residues and stones as well as other impurities visible to the naked eye, and then used for the determination of soil physicochemical properties and humus carbon fractions.

2.4. Soil Analysis

2.4.1. Soil Physicochemical Property Analysis

The soil bulk density (BD) and field water holding capacity (WHC) were determined by drilling soil cores using the core ring method [31]. Soil pH was measured using a digital pH meter at a soil/water ratio of 1:2.5. The content of nitrate (NO_3^- -N) and ammonium (NH_4^+ -N) was determined using an automatic discrete analyzer (Westco SmartChem 200, AMS Alliance, Rome, Italy). Alkaline nitrogen (AN) was determined using the alkaline hydrolysis diffusion method [32]. Total phosphorus (TP) and available phosphorus (AP) were determined using the NaOH fusion–molybdenum antimony anti-colorimetric method [33]. The total potassium (TK) and available potassium (AK) were determined by flame photometry after fusion with NaOH and extraction with 1.0 mol L^{-1} of NH_4OAc [34].

2.4.2. Soil Aggregate Isolation

Isolation of soil water-stable aggregates was performed according to the method of Kemper and Rosenau [35]. Using a water-stable aggregate analyzer, 50 g of the air-dried soil samples was weighed, passed through 2, 0.25, and 0.053 mm sieve apertures in that order, from top to bottom, immersed in distilled water for 5 min, and then automatically shaken up and down at 30 r min^{-1} for 2 min (amplitude of 3 cm). Soil aggregate fractions were oven-dried to a constant weight of $60 \text{ }^\circ\text{C}$ and then weighed. Soil water-stable aggregates were isolated into four different fraction sizes: (1) large macroaggregates (diameter $> 2 \text{ mm}$); (2) small macroaggregates (diameter of $2\text{--}0.25 \text{ mm}$); (3) microaggregates (diameter of $0.25\text{--}0.053 \text{ mm}$); (4) silt + clay (diameter $< 0.053 \text{ mm}$).

2.4.3. Organic and Humus Carbon Measurements in Bulk Soils and Water-Stable Aggregate Fractions

Organic carbon concentrations of bulk soil and aggregate fractions sieved through a 0.15 mm mesh were measured using an elemental analyzer (EA 3000, Euro Vector, Rome, Italy). Extraction, fractionation, and purification of soil humic substance fractions were carried out according to the method of Rivero et al. [36]. Samples (5 g) of bulk soil and aggregate fractions were weighed and passed through a 60 mesh sieve in a 100 mL centrifuge tube, to which 50 mL of a mixed 0.1 M NaOH and 0.1 M $\text{Na}_4\text{P}_2\text{O}_7$ solution was added and extracted by incubating the sample in a $70 \text{ }^\circ\text{C}$ constant-temperature oscillating water bath for 1 h. Next, the sample was centrifuged at 3500 r min^{-1} for 15 min, and the filtrate was the extraction of humic substances (HE). The residues in the centrifuge tube were washed with distilled water and dried at $60 \text{ }^\circ\text{C}$ and represent humin (HM). The next day, the solution was filtered and calibrated in 50 mL volumetric bottles to collect acid-soluble fulvic acids (FAs). The concentration was fixed in distilled water and represents acid-insoluble humic acids (HAs). Fulvic acid carbon (FAC) was calculated by subtracting HAC from HEC, while humin carbon (HUC) was calculated by subtracting the sum of HAC and FAC from the SOC.

2.5. Calculation and Statistical Analysis

The content of the soil aggregate fractions was calculated according to the description from Elliott [37], as follows:

$$R_i = \frac{w_i}{50} \quad (1)$$

where R_i represents the percentage of soil aggregates of each size (%), and W_i represents the quantity of the soil aggregates of this size (g).

The stability of the soil aggregates was evaluated by calculating the mean weight diameter (MWD), the geometric mean diameter (GMD), and the percentage of macroaggregates ($R > 0.25$ mm).

$$\text{MWD} = \frac{\sum_{i=1}^n \bar{X}_i W_i}{\sum_{i=1}^n W_i} \quad (2)$$

$$\text{GMD} = \text{EXP} \left[\frac{\sum_{i=1}^n W_i \ln \bar{x}}{\sum_{i=1}^n W_i} \right] \quad (3)$$

$$R_{>0.25} = \frac{M_{>0.25}}{50} \quad (4)$$

where X_i is the mean diameter of aggregates of each particle size (mm), W_i is the percentage content of aggregates of each particle size (%), and $M > 0.25$ mm is the weight of the macroaggregates (g).

Pearson's correlation analysis was employed to reveal the relationship among grain yield, soil physicochemical properties, and humic carbon pool. The differences in comparisons between treatments were detected using one- and two-way analyses of variance (ANOVAs) and Duncan's multiple range tests (Duncan's) at the 0.05 level of probability ($p < 0.05$). All data were analyzed using the analytical package SPSS Statistics 23.0 software (SPSS Inc., Chicago, IL, USA) for comparison of differences among treatments, while Origin 9.0 software (Origin Lab Inc., Northampton, MA, USA) was used for the correlation analyses and preparing graphs.

Structural equation modeling (SEM) analysis was conducted using AMOS (IBM SPSS AMOS 23, Chicago, IL, USA) software developed by IBM. The model was used to explore the direct and indirect effects of the humus carbon fractions in aggregates of each particle size, the organic carbon in the aggregate fractions, and the humus carbon in the bulk soil on soil organic carbon sequestration. Our aim is to find the transformation pathways from carbon molecules at the soil microgranular level to organic and humus carbon macromolecules, which may contribute more to our understanding of the relationship between the various fractional aggregate sizes and soil carbon sequestration. Finally, the path coefficients between the variables were calculated using the maximum likelihood method by AMOS 23 software. Standardized path coefficients were selected based on the range of values (−1 to 1) and significance ($p < 0.05$) between the two variables, together with the removal of nonsignificant paths. The structural equation model final fitting was determined using a nonsignificant chi-square test and its associated p -value ($p > 0.05$), comparative fit index (CFI), the goodness of fit index (GFI), and root mean square error of approximation (RMSEA).

3. Results

3.1. Soil Physicochemical Properties in Different Straw Return Modes

In the 0–10 cm layer, tillage (T) and straw management (S) had significant effects on the AK, TN, and NO_3^- -N contents and pH ($p < 0.05$) (Table 1). Further analysis revealed that PTS significantly decreased BD and increased soil pH compared to the other treatments. In the 10–20 cm layer, both tillage and straw management, as well as their interaction, significantly affected the AN, AK, TN, and NO_3^- -N contents and pH ($p < 0.05$) (Table 1). In the 20–30 cm layer, tillage, straw management, and their interaction had significant effects on the BD, AP, AK, and NO_3^- -N contents and pH ($p < 0.05$) (Table 1).

Table 1. Effect of tillage and straw return mode on the physicochemical properties of the soil layer.

Soil Depth (cm)	Straw Return Mode	BD (g·cm ³)	WHC (%)	AN (mg·kg ⁻¹)	AP (mg·kg ⁻¹)	AK (mg·kg ⁻¹)	TN (g·kg ⁻¹)	TP (g·kg ⁻¹)	TK (g·kg ⁻¹)	NH ₄ ⁺ -N (mg·kg ⁻¹)	NO ₃ ⁻ -N (mg·kg ⁻¹)	pH
0–10	RTS	1.22 a	33.63 a	108.42 ab	12.91 d	193.64 b	1.24 b	0.47 a	19.68 ab	8.12 ab	7.40 d	5.00 b
	PTS	1.09 b	32.59 a	102.36 b	17.52 c	183.48 c	1.22 b	0.42 a	18.48 b	7.30 b	8.49 c	5.13 a
	RSS	1.18 a	35.11 a	138.94 a	21.62 a	210.08 a	1.39 a	0.55 a	21.09 a	8.87 a	15.33 a	4.84 d
	PSS	1.18 a	35.18 a	118.38 ab	19.07 b	192.44 b	1.20 b	0.42 a	20.86 a	6.89 b	9.68 b	4.88 c
	ANOVA											
	T	*	ns	ns	ns	**	**	ns	ns	**	**	**
	S	ns	ns	*	**	**	*	ns	**	ns	**	**
T × S	*	ns	ns	**	ns	*	ns	ns	ns	**	**	
10–20	RTS	1.37 a	31.14 a	99.52 b	12.87 d	155.91 b	1.01 d	0.50 a	21.90 a	6.00 d	5.84 d	5.18 b
	PTS	1.31 ab	31.99 a	80.58 c	14.66 c	136.39 c	1.14 c	0.37 b	22.71 a	9.51 b	7.57 c	5.58 a
	RSS	1.22 b	37.41 a	109.72 a	17.88 a	159.51 a	1.24 a	0.50 a	23.11 a	10.62 a	21.62 a	4.96 c
	PSS	1.28 ab	35.55 a	106.47 ab	16.98 b	156.39 b	1.20 b	0.43 b	21.52 a	6.70 c	9.24 b	5.14 b
	ANOVA											
	T	ns	ns	**	ns	**	**	**	ns	ns	**	**
	S	ns	ns	**	**	**	**	ns	ns	**	**	**
T × S	ns	ns	**	**	**	**	ns	ns	**	**	**	
20–30	RTS	1.52 a	26.61 a	74.23 b	3.80 b	114.06 c	0.95 a	0.36 a	21.66 a	3.45 c	5.45 c	5.45 d
	PTS	1.38 b	27.13 a	84.38 ab	1.94 c	103.13 d	0.94 a	0.34 a	21.81 a	6.26 b	7.53 b	6.29 a
	RSS	1.37 b	30.73 a	93.89 ab	4.79 a	119.75 b	0.96 a	0.36 a	22.66 a	9.21 a	8.33 a	6.19 b
	PSS	1.37 b	30.47 a	106.91 a	4.67 a	149.29 a	0.95 a	0.35 a	20.17 a	7.27 b	7.24 b	6.06 c
	ANOVA											
	T	**	ns	ns	**	**	ns	ns	ns	ns	*	**
	S	**	*	*	**	**	ns	ns	ns	**	**	**
T × S	**	ns	ns	**	**	ns	ns	ns	**	**	**	

T, tillage; S, straw management; T × S, Interaction of tillage and straw management. RTS, rotary tillage with straw return; PTS, plow tillage with straw return; RSS, rotary tillage with straw strip return; PSS, plow tillage with straw strip return. The tillage layer (0–30 cm) was divided into three layers: topsoil (0–10 cm), mid-soil (10–20 cm) and subsoil (20–30 cm), respectively. BD, bulk density; WHC, field water holding capacity; AN, alkaline nitrogen; AP, available phosphorus; AK, available potassium; TN, total nitrogen; TP, total phosphorus; TK, total potassium; pH, acidity and alkalinity; NH₄⁺-N, ammonium nitrogen; NO₃⁻-N, nitrate nitrogen. Values represent the means of three replicates. Different lowercase letters indicate significant differences ($p < 0.05$) between tillage and straw return mode treatments. * indicates significant difference ($p < 0.05$), ** indicates extremely significant difference ($p < 0.01$), ns indicates not significant.

3.2. Organic and Humus Carbon Concentrations in Bulk Soil

Tillage (T) and straw management (S), as well as their interaction (T × S), had significant effects on the SOC content in the 0–10 cm and 20–30 cm layers ($p < 0.05$), whereas in the 10–20 cm layer, no significant difference was observed for their interaction (Figure 2A). In the 0–10 cm and 10–20 cm layers, straw management had a significant effect on the HAC content ($p < 0.05$); however, in the 20–30 cm layer, the interaction of tillage and straw management had no significant effect on the HAC content (Figure 2B). Furthermore, both the FAC and HMC contents were higher in RSS than in PTS, RTS, and PSS at each depth (Figure 2C,D).

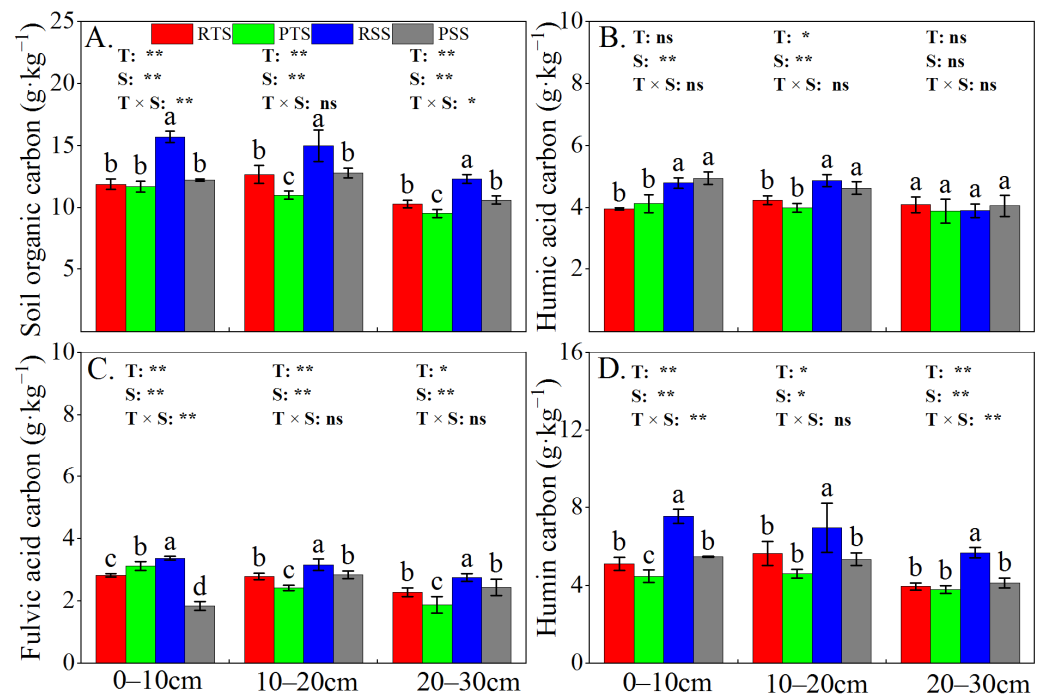


Figure 2. Concentrations of organic and humus carbon fractions in bulk soil under different tillage and straw return modes. (A) soil organic carbon (SOC); (B) humic acid carbon (HAC); (C) fulvic acid carbon (FAC); (D) humin carbon (HUC). RTS, rotary tillage with straw return; PTS, plow tillage with straw return; RSS, rotary tillage with straw strip return; PSS, plow tillage with straw strip return. The tillage layer (0–30 cm) was divided into three layers: topsoil (0–10 cm), mid-soil (10–20 cm) and subsoil (20–30 cm), respectively. Error bars represent the standard deviations of the mean ($n = 3$). Different lowercase letters indicate significant differences between treatments ($p < 0.05$). T, tillage; S, straw management; * indicates significant difference ($p < 0.05$), ** indicates extremely significant difference ($p < 0.01$), ns indicates not significant.

3.3. Soil Aggregate Size Distribution and Stability

In the 0–10 cm layer, RSS significantly increased large macroaggregates (149.2%, 167.5%, and 125.3%) and small macroaggregates (35.3%, 19.7%, and 14.5%) but decreased the microaggregate (35.31%, 44.71%, and 36.93%) and silt/clay (61.92%, 42.54%, and 45.26%) contents compared to RTS, PTS, and PSS, respectively. Tillage, straw management, and their interaction had significant effects on the distribution of large macroaggregates and microaggregates (Figure 3A). Similarly, in the 10–20 cm layer, a higher large macroaggregate content (19.7%, 180.9%, and 151.3%) and a lower silt/clay content (53.54%, 75.07%, and 57.76%) were observed compared to RTS, PTS, and PSS, respectively. However, the interaction between tillage and straw management was not significant ($p < 0.05$).

As shown in Table 2, tillage and straw management significantly regulated the stability of soil water-stable aggregates, and the effect of tillage and straw management was significant in the 0–10 cm layer ($p < 0.05$). Specifically, RSS significantly increased the

proportion of $R_{0.25\text{ mm}}$ at depths of 0–10 cm (61.1%, 48.4%, and 38.3%) and 10–20 cm (18.9%, 71.2%, and 26.9%) compared to RTS, PTS, and PSS. This is consistent with the trend of MWD and GMD as compared to the other treatments, with increased MWD (64.1%, 54.4%, and 40.0%) and GMD (124.1%, 85.71%, and 62.5%) in the 0–10 cm layer and MWD (13.3%, 61.9%, and 30.8%) and GMD (25.53%, 110.7% and 40.48%) in the 10–20 cm layer observed under RSS treatment.

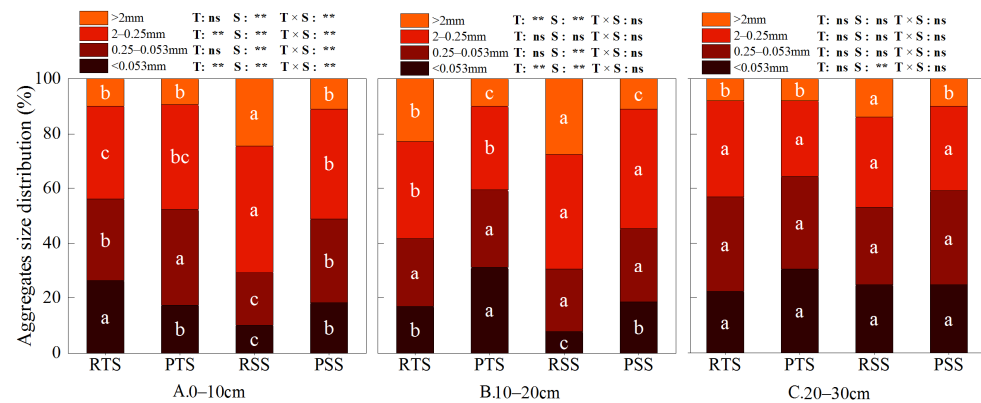


Figure 3. The distribution of water-stable aggregate fractions in soil under different tillage and straw return modes. RTS, rotary tillage with straw return; PTS, plow tillage with straw return; RSS, rotary tillage with straw strip return; PSS, plow tillage with straw strip return. (A) indicates topsoil (0–10 cm), (B) indicates mid-soil (10–20 cm), and (C) indicates subsoil (20–30 cm), respectively. Error bars represent the standard deviations of the mean ($n = 3$). Different lowercase letters indicate significant differences between treatments ($p < 0.05$). T, tillage; S, straw management; ** indicates extremely significant difference ($p < 0.01$), ns indicates not significant.

Table 2. Effect of tillage and straw return mode on the stability of soil water-stable aggregates.

Straw Return Mode	$R_{0.25\text{ mm}}$ (%)			MWD (mm)			GMD (mm)		
	0–10 cm	10–20 cm	20–30 cm	0–10 cm	10–20 cm	20–30 cm	0–10 cm	10–20 cm	20–30 cm
RTS	43.88 c	58.30 b	43.13 ab	0.64 b	0.90 b	0.62 ab	0.29 c	0.47 b	0.30 a
PTS	47.63 bc	42.81 c	35.76 b	0.68 b	0.63 d	0.54 b	0.35 bc	0.28 c	0.24 a
RSS	70.67 a	65.97 a	46.98 a	1.05 a	1.02 a	0.71 a	0.65 a	0.59 a	0.33 a
PSS	54.09 b	59.29 b	40.91 ab	0.75 b	0.78 c	0.61 ab	0.40 b	0.42 b	0.28 a
ANOVA									
T	*	**	*	**	**	*	**	**	ns
S	**	**	ns	**	**	*	**	**	ns
T × S	**	ns	ns	**	ns	ns	**	ns	ns

T, tillage; S, straw management; T × S, Interaction of tillage and straw management. RTS, rotary tillage with straw return; PTS, plow tillage with straw return; RSS, rotary tillage with straw strip return; PSS, plow tillage with straw strip return. The tillage layer (0–30 cm) was divided into three layers: topsoil (0–10 cm), mid-soil (10–20 cm) and subsoil (20–30 cm), respectively. $R_{0.25\text{ mm}}$, the proportion of macroaggregates with diameter $>0.25\text{ mm}$; MWD, mean weight diameter; GMD, geometric mean diameter. Values represent the means of three replicates. Different lowercase letters indicate significant differences ($p < 0.05$) between tillage and straw return mode treatments. * indicates significant difference ($p < 0.05$), ** indicates extremely significant difference ($p < 0.01$), ns indicates not significant.

3.4. Organic and Humus Carbon Concentrations in Aggregate Fractions

Tillage had a significant effect on the aggregate organic C in all soil layers from 0 to 30 cm ($p < 0.05$), except for large macroaggregates and microaggregates in the 0–10 cm layer (Table 3). Therefore, the small macroaggregate and silt + clay-associated organic C concentrations in RTS and RSS were significantly higher than in PTS and PSS, respectively (Figure 4A). Furthermore, RSS had significantly higher HAC concentrations than RTS, PTS, and PSS at depths of 0–10 cm and 20–30 cm associated with all aggregate sizes (Figure 4D,F). However, at a depth of 10–20 cm, the HAC concentrations in PTS aggregates were significantly higher than those of the other treatments (Figure 4E).

Table 3. Interaction of tillage and straw management on aggregate size-associated organic and humus carbon.

Aggregate Carbon Fractions	ANOVA	0–10 (cm)				10–20 (cm)				20–30 (cm)			
		>2	2–0.25	0.25–0.053	<0.053	>2	2–0.25	0.25–0.053	<0.053	>2	2–0.25	0.25–0.053	<0.053
		(mm)											
SOC (F)	T	1.32 ^{ns}	36.08 ^{**}	4.99 ^{ns}	36.85 ^{**}	2.75 ^{ns}	29.25 ^{**}	24.54 ^{**}	20.39 ^{**}	37.87 ^{**}	37.82 ^{**}	24.48 ^{**}	80.21 ^{**}
	S	0.001 ^{ns}	0.04 ^{ns}	1.49 ^{ns}	0.12 ^{ns}	0.00 ^{ns}	0.38 ^{ns}	3.50 ^{ns}	1.54 ^{ns}	0.75 ^{ns}	2.85 ^{ns}	0.68 ^{ns}	0.37 ^{ns}
	T × S	3.434 ^{ns}	1.81 ^{ns}	0.86 ^{ns}	2.71 ^{ns}	10.16 [*]	51.29 ^{**}	5.05 ^{ns}	20.35 ^{**}	30.04 ^{**}	4.62 ^{ns}	0.91 ^{ns}	0.62 ^{ns}
HAC (F)	T	162.48 ^{**}	207.16 ^{**}	196.54 ^{**}	75.66 ^{**}	53.04 ^{**}	36.73 ^{**}	18.31 ^{**}	2.87 ^{ns}	92.01 ^{**}	102.98 ^{**}	61.93 ^{**}	3.45 ^{ns}
	S	110.98 ^{**}	91.26 ^{**}	69.64 ^{**}	7.18 [*]	83.34 ^{**}	466.49 ^{**}	65.37 ^{**}	217.30 ^{**}	18.67 ^{**}	55.29 ^{**}	20.73 ^{**}	5.28 ^{ns}
	T × S	18.37 ^{**}	0.35 ^{ns}	2.29 ^{ns}	0.66 ^{ns}	26.10 ^{**}	106.75 ^{**}	18.07 ^{**}	20.67 ^{**}	54.51 ^{**}	30.58 ^{**}	35.27 ^{**}	8.85 [*]
FAC (F)	T	144.74 ^{**}	17.37 ^{**}	154.71 ^{**}	63.22 ^{**}	41.55 ^{**}	86.65 ^{**}	37.35 ^{**}	69.99 ^{**}	438.97 ^{**}	149.90 ^{**}	199.04 ^{**}	110.13 ^{**}
	S	2.69 ^{ns}	2.51 ^{ns}	24.87 ^{**}	0.03 ^{ns}	96.73 ^{**}	2.23 ^{ns}	27.29 ^{**}	85.70 ^{**}	126.81 ^{**}	55.30 ^{**}	283.95 ^{**}	67.44 ^{**}
	T × S	272.92 ^{**}	241.10 ^{**}	397.94 ^{**}	225.80 ^{**}	233.54 ^{**}	201.97 ^{**}	469.92 ^{**}	145.27 ^{**}	472.98 ^{**}	113.69 ^{**}	263.02 ^{**}	38.68 ^{**}
HMC (F)	T	1.69 ^{ns}	17.02 ^{**}	2.02 ^{ns}	27.37 ^{**}	13.53 ^{**}	90.25 ^{**}	80.26 ^{**}	42.96 ^{**}	1.50 ^{ns}	24.66 ^{**}	17.89 ^{**}	4.47 ^{ns}
	S	1.24 ^{ns}	12.29 ^{**}	18.19 ^{**}	5.48 [*]	0.42 ^{ns}	10.35 [*]	17.91 ^{**}	0.11 ^{ns}	242.85 ^{**}	19.76 ^{**}	94.64 ^{**}	58.17 ^{**}
	T × S	0.55 ^{ns}	34.15 ^{**}	16.57 ^{**}	87.01 ^{**}	17.10 ^{**}	148.73 ^{**}	32.02 ^{**}	36.02 ^{**}	7.96 [*]	0.40 ^{ns}	7.27 [*]	5.40 [*]

T, Tillage; S, Straw management; T × S, Interaction of tillage and straw management. Large macroaggregates, >2 mm; Small macroaggregates, 2–0.25 mm; Microaggregates, 0.25–0.053 mm; Silt + clay, <0.053 mm. The tillage layer (0–30 cm) was divided into three layers: topsoil (0–10 cm), mid-soil (10–20 cm) and subsoil (20–30 cm), respectively. SOC, Soil organic carbon; HAC, Humic carbon; FAC, Fulvic acid carbon; HMC, Humin carbon. * indicates significant difference ($p < 0.05$), ** indicates extremely significant difference ($p < 0.01$), ^{ns} indicates not significant.

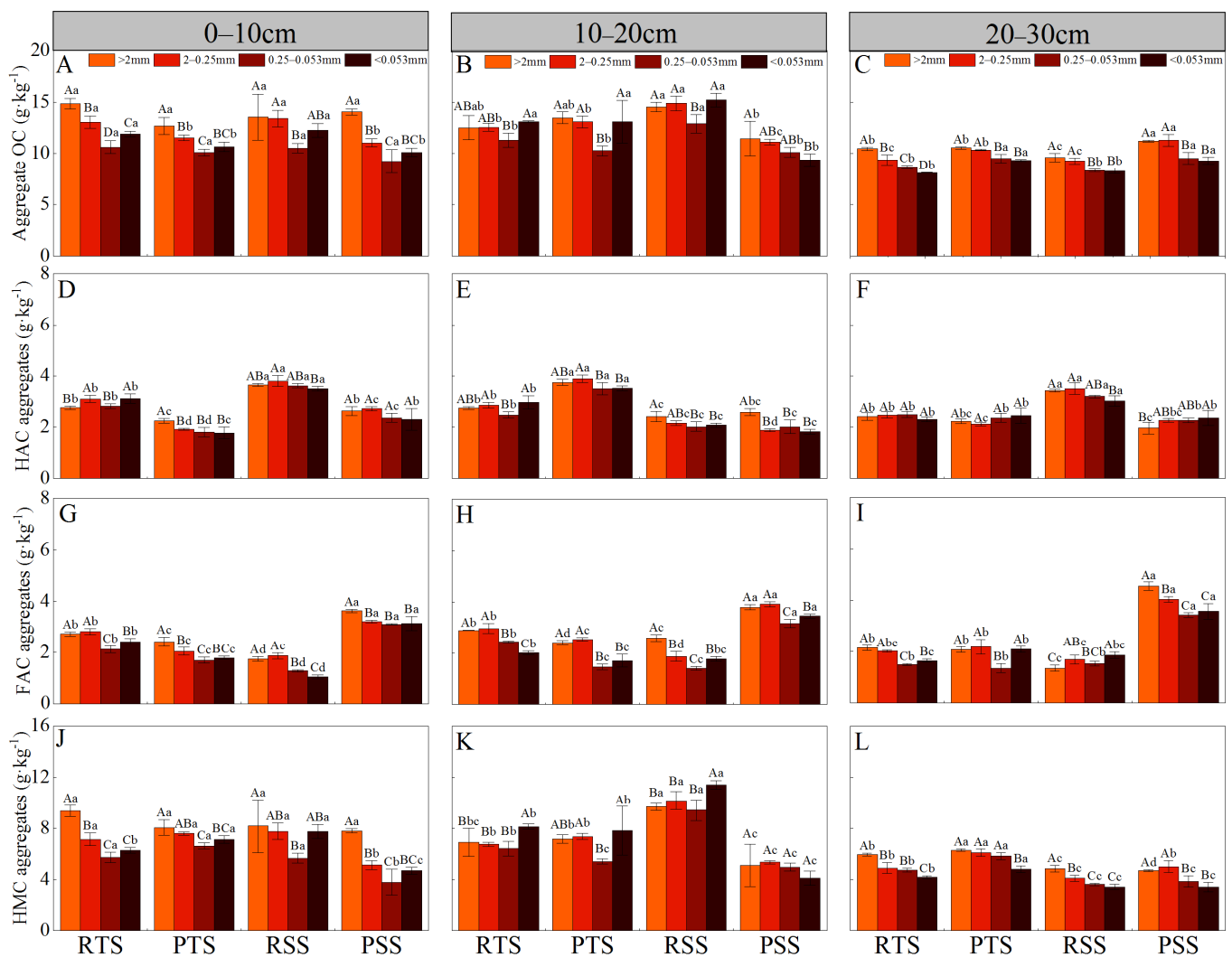


Figure 4. The organic carbon (OC) and humus carbon concentrations of the water-stable aggregate fractions under different tillage and straw return modes. (A) aggregate OC at 0–10 cm soil depths; (B) aggregate OC at 10–20 cm soil depths; (C) aggregate OC at 20–30 cm soil depths; (D) HAC aggregate at 0–10 cm soil depths; (E) HAC aggregate at 10–20 cm soil depths; (F) HAC aggregate at 20–30 cm soil depths; (G) FAC aggregate at 0–10 cm soil depths; (H) FAC aggregate at 10–20 cm soil depths; (I) FAC aggregate at 20–30 cm soil depths; (J) HMC aggregate at 0–10 cm soil depths; (K) HMC aggregate at 10–20 cm soil depths; (L) HMC aggregate at 20–30 cm soil depths. RTS, rotary tillage with straw return; PTS, plow tillage with straw return; RSS, rotary tillage with straw strip return; PSS, plow tillage with straw strip return. Error bars represent the standard deviations of the mean ($n = 3$). Different capital letters indicate significant differences ($p < 0.05$) between organic and humus carbon associated with different aggregate sizes within the same treatment. Different lowercase letters indicate significant differences between treatments ($p < 0.05$). T, tillage; S, straw management.

Tillage and the interaction of $T \times S$ had significant effects on FAC associated with all aggregate sizes in the 0–10 cm layer ($p < 0.05$), whereas tillage, straw management, and their interaction had significant effects ($p < 0.05$) on FAC associated with all aggregate sizes in the 10–20 and 20–30 cm layers (Table 3). PSS significantly increased FAC associated with all aggregate sizes in all layers from 0 to 30 cm depth (Figure 4G–I). Tillage, straw management, and their interaction had significant effects on small macroaggregate- and silty/clay-associated HMC in the 0–10 cm layer, small macroaggregate- and microaggregate-associated HMC in the 10–20 cm layer, and microaggregate-associated HMC in the 20–30 cm

layer (Table 3). At a depth of 10–20 cm, RSS significantly increased all aggregate size-associated HMC concentrations compared to RTS, PTS, and PSS (Figure 4K).

3.5. Correlation Analysis between Physicochemical Properties and Organic and Humus Carbon

Correlation analysis showed that in the topsoil, soil property indicators (AP, AK, TN, TK, and FAs) were negatively correlated with the FAC of the aggregate fractions. The HAC of the aggregate fractions was positively correlated with AK, TN, NH_4^+ -N, and SOC and negatively correlated with BD (Figure 5A). The HAC of the aggregate fractions showed a highly significant positive correlation with pH ($p < 0.001$) and a negative correlation with AK, SOC, and FAs (Figure 5B). The HAC and FAC of the aggregate fractions were positively correlated with AK ($p < 0.001$) in the subsoil. The HMC of the aggregate particles showed a highly significant negative correlation with AP ($p < 0.001$), but a significant positive correlation with the HM ($p < 0.05$). The SOC of the aggregate fractions was positively correlated with AK and pH ($p < 0.05$) (Figure 5C). Still, the pH and HMC of the aggregate particles were negatively correlated with yield in the subsoil.

3.6. Model Analysis on the Transformation of Organic and Humus Carbon

Structural equation modeling (SEM) was used to finally establish a model according to the results of data fitting ($\chi^2/\text{df} = 1.09$, $p = 0.337$, RMSEA = 0.05, GFI = 0.99, CFI = 1.00). According to SEM analysis, the total variation in organic and humus carbon in the bulk soil comprising SOC was 100%; meanwhile, HAs was 81%, FAs was 74%, and HM was 85% (Figure 6). Worth noting is that only the microaggregates and the silt + clay negatively affected FAs and HM (path coefficients of -0.41 and -0.52 , respectively). The FAclay directly affected the SOCmicro (path coefficient of 0.66), while the HMclay affected the SOCsmall and SOCmicro (path coefficients of 0.41 and 0.60, respectively), in addition to the HM (path coefficient of 0.55). The pattern of SOC turnover within the aggregates was determined as follows: First, the small macroaggregates are decomposed into microaggregates (path coefficient of 0.47), further decomposed into silt + clay (path coefficient of 0.44), and then utilize the cementation of silt + clay to reform large macroaggregates (path coefficient of 0.51). Interestingly, the SOC in silt + clay and the HAs in bulk soil were found to be strongly correlated (path coefficient of 0.90). Among the direct effects of the humus carbon fractions on the SOC, HM had the strongest influence (path coefficient of 0.66), followed by FAs and HAs (path coefficients of 0.27 and 0.24, respectively). In addition, HAs had a significantly greater impact on HM than FAs (path coefficients of 0.73 and 0.42, respectively) and indirectly promoted SOC accumulation. Through structural equation modeling, we identified intermediate carriers of soil carbon sequestration, namely FAclay, HMclay, SOCsmall, SOCmicro, SOCclay, HAs, and HM. The aggregate size-associated humus carbon fractions were eventually significantly enriched in the HAs (81%) and HM (85%) of bulk soil through a series of transformations and revolutions and ultimately immobilized into the soil as organic carbon (Figure 6).

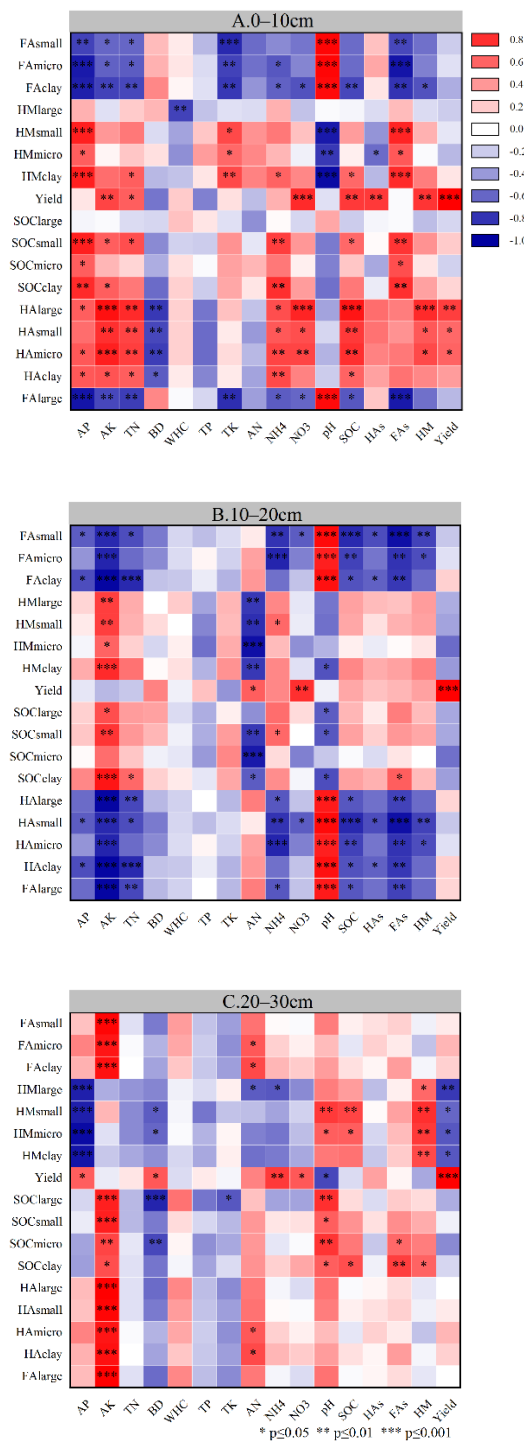


Figure 5. Pearson’s rank correlation coefficients between soil physicochemical properties and aggregates stability and maize grain yield and concentration of humus carbon pool at different depths of the soil layer. (A) indicates topsoil (0–10 cm), (B) indicates mid-soil (10–20 cm), and (C) indicates subsoil (20–30 cm), respectively. (*) Correlation is significant at the 0.05 level; (**) Correlation is significant at the 0.01 level; (***) Correlation is significant at the 0.001 level. BD, bulk density; WHC, field water holding capacity; AN, alkaline nitrogen; AP, available phosphorus; AK, available potassium; TN, total nitrogen; TP, total phosphorus; TK, total potassium; SOC, soil organic carbon; pH, acidity and alkalinity; NH₄⁺-N, ammonium nitrogen; NO₃⁻-N, nitrate nitrogen; HAs, humic acids; FAs, fulvic acids; HM, humin; large, large-macroaggregate; small, small-macroaggregate; micro, microaggregates; clay, silt and clay.

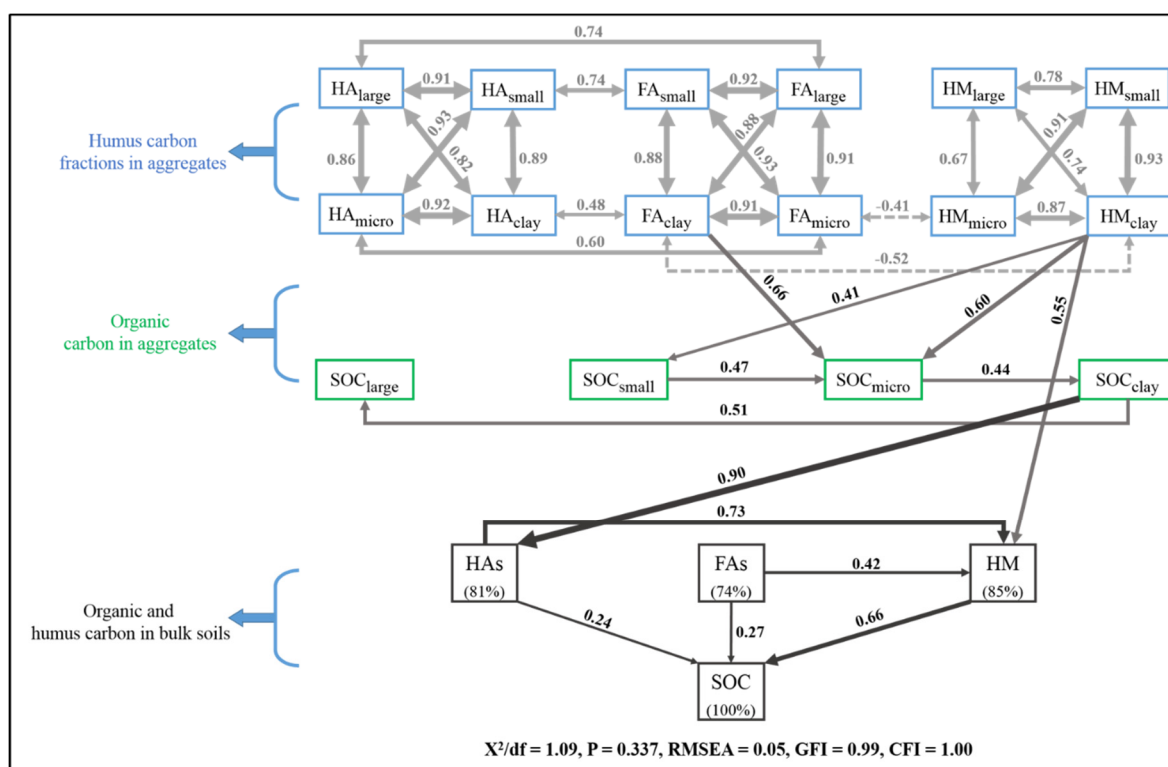


Figure 6. Structural equation model showing the direct and indirect effects of soil organic carbon (SOC), humic acids (HAs) carbon, fulvic acids (FAs) carbon and humin (HM) carbon within aggregates on organic and humus carbon in bulk soil. Note, the solid and dashed arrows represent the positive and negative relationships between variables, respectively. The number on the arrow represents the standardized path coefficient, the thickness of the arrow indicates the magnitude of the path coefficient, and the percentage is the total variance explained by the model.

4. Discussion

4.1. Effects of Straw Return Mode on Physicochemical Properties and Aggregate Stability

The tillage with straw strip return mode is defined as a reduced form of tillage because it does not disturb the whole soil cultivated layer, i.e., conservation strip-till [21]. In this study, RSS and PSS increased the available nutrient contents (AN, AP, and AK) at depths of both 0–10 cm and 10–20 cm (Table 1) compared to RTS and PTS, respectively. This could be because reduced and no-tillage combined with straw return practices enhance SOC sequestration, indirectly promoting abiotic factor properties, accelerating straw nutrient release (mainly N, P, and K), and further improving the physicochemical environment [38,39].

A recent meta-analysis indicated, conservation tillage combined with straw return can either increase or decrease the soil bulk density, bulk density values would not exceed the threshold ($BD > 1.40 \text{ g cm}^{-3}$) that limits crop growth [21,40]. Therefore, this was consistent with our results, in which the values of bulk density in all return modes were less than 1.40 g cm^{-3} , and only the control (RTS) using conventional tillage exceeded the limit threshold of 8.57% at a depth of 20–30 cm (Table 1). It is well known that water-stable aggregate stability and aggregate size distribution are effective indicators for use in the comprehensive assessment of soil structural quality [21]. Among them, the mass proportion of macroaggregates, MWD, and GMD reflect aggregate stability, whereby higher values indicate greater stability [41,42]. The same results were found by Wang et al. [23] in a nine-year experiment, which indicated a significant increase in MWD, GMD, and the proportion of macroaggregates in the tillage layer with reduced/no-tillage combined with straw return compared to RTS and PTS [43,44].

RSS significantly increased the contents of SOC, FAC, and HMC in all soil layers from 0 to 30 cm (Figure 2A,C,D) as well as the proportion of large macroaggregates (Figure 3A–C). Additionally, it significantly increased the soil aggregate stability at depths of 0 to 20 cm compared to the other treatments (Table 2). This might be due to, first, strip rotary tillage being similar to reduced tillage practices with minimal soil disturbance, maintaining an excellent aggregation structure and, combined with the total straw return, increasing the surface SOC content, thus promoting soil aggregate formation [45,46]. Second, straw return increased the proportion of macroaggregates, enriched with soil organic matter and moderated soil moisture and temperature fluctuations in the surface layer, while decreasing aggregate wettability and turnover rates, thereby better increasing aggregate stability and protecting against aggregate disintegration [47,48]. Therefore, these findings contribute to further illuminating the mechanisms of accumulation in different humus carbon fractions of soil under strips of straw return. Overall, RSS improved soil physicochemical properties, due to the minimal disturbance and sufficient mixing of topsoil with straw, resulting in increased soil nutrient content and aggregation.

Furthermore, Figure S2 showed that a lower maize yield was observed in 2018 compared to other years, which was caused by extreme weather during the growing season (Figure S1). Based on a five-year average, the maize grain yield was significantly higher under the RSS and PSS treatments than under the PTS and RTS treatments. This trend was consistent with the soil physicochemical properties, indicating that straw strip return plays an important role in ensuring food security.

4.2. Structural Equation Modeling and Transformation Mechanisms of Organic and Humus Carbon

RSS had significantly higher aggregate-associated HAC concentrations than the other treatments (Figure 4D,F). In contrast, higher aggregate-associated HMC concentrations were found at a depth of 10–20 cm (Figure 4K). This might be because RSS decreased soil disturbance, resulting in improved soil physicochemical properties and aggregate stability, which indirectly promoting the accumulation of HAC and HMC in the soil, thus promoting soil microbial activity at different depths. Therefore, HAC and HMC play a crucial role in the accumulation of aggregate-size-associated organic carbon in RSS. Specifically, the mechanisms underlying SOC stabilization are related to the (i) chemical recalcitrance of HAs, which is highly protective of SOC due to its high aromaticity and aliphatic and alkyl carbon contents, thus promoting hydrophobicity; and (ii) association of HMC with soil minerals, which has the largest molecular weight among humus fractions, with a highly insoluble, viscous, and inert texture that allows it to strongly bind to clay minerals, iron–aluminum oxides, and metal cations, and it is the most decomposition-resistant cementing agent in soil [49]. Among all soil layers from 0 to 30 cm, the aggregate-associated organic carbon fractions of PSS were significantly enriched with FAC (Figure 5G–I). The main components of FAC are unstable water-soluble compounds, such as polysaccharides and proteins, which are the main components of soil labile organic carbon. Some studies have indicated that fulvic acid is a precursor of the humus fraction, and when straw humification forms humus, the fulvic acids content is significantly increased [50].

This study indicates that the transformation between organic and humus carbon fractions within aggregates has different pathways (Figure 6). Therefore, the transformation process of aggregate-associated humus carbon fractions to aggregate-associated organic carbon, to humus carbon fractions in bulk soil, and to soil organic carbon was simulated using structural equation modeling (SEM). We clearly observed high path coefficients for HAC and FAC at the same aggregate size, as well as for HAC or FAC between different aggregate sizes (Figure 6). Since HAC and FAC are formed by humic substrates heated by acids and alkalis that are filtered, there is a correlation between the two in terms of material composition and nutrient exchange, so the interconversion coefficient is greater [51]. In contrast, HMC does not exchange materials with HAC and FAC due to its higher chemical recalcitrance and [49], surprisingly, a significant negative correlation was observed between HMC and FAC in microaggregates and silts/clays.

Furthermore, small macroaggregates and microaggregates are the main transporters of aggregate-associated humus carbon fractions, and previous studies have indicated that small macroaggregates and microaggregates are the most abundant of the different sized aggregates in soils, in which they are important components facilitating organic carbon accumulation [47]. Subsequently, SOC was further decomposed and bound between aggregates of varying size and eventually accumulated in the HAC and HMC in bulk soil. SEM revealed the contribution of HAC and HMC to SOC was 81% and 85%, respectively, thus confirming our previous hypothesis that humic acid and humin play a predominant role in organic carbon sequestration [48,52]. Through SEM prediction of the transformation relationships between organic and humus carbon molecules, we have clarified the effects of these components on soil carbon sequestration (FAclay, HMclay, SOCsmall, SOCmicro, SOCclay, HAs, and HM, respectively). Although we defined these components through model simulations, this is only a link between quantitative relationships and may not be sufficient for illuminating the real situation between organic and humus carbon in aggregate sizes. Therefore, this will be a challenge in our future study and we need to find other real data to confirm our conclusions. It is known from previous studies that the structural composition of soil carbon molecules can be accurately defined using advanced ^{13}C NMR spectroscopy, which may play a crucial role in our future study [28].

5. Conclusions

In our study, tillage and straw return were found to affect soil physicochemical properties, aggregate stability, and SOC sequestration. Specifically, RSS increased the SOC concentration at a depth of 0–30 cm, and the significant improvement in SOC could be attributed to the enrichment of the humus carbon fractions of HMC and FAC. The proportion of macroaggregates (>0.25 mm) and aggregate stability (MWD and GMD) were higher for RSS treatment, resulting in an effective improvement in soil structure and facilitating straw humification and SOC sequestration. Structural equation modeling (SEM) revealed that silt/clay-associated FAC and HMC are involved in soil C turnover within aggregates, and ultimately contribute to the accumulation of HAC and HMC in soil, thereby promoting SOC sequestration. Our results demonstrate that RSS is a more suitable system for optimizing soil macroaggregates toward increasing the humus C content of cultivated land and long-term stabilization of soil C in Mollisols of Northeast China.

Supplementary Materials: The following supporting information can be downloaded at: <https://www.mdpi.com/article/10.3390/agronomy12040784/s1>, Figure S1: The mean daily temperature and precipitation from May to September during the Maize growing season in 2015 to 2019; Figure S2: Maize grain yield during the period of 2015 to 2019 between different straw return modes.

Author Contributions: Conceptualization, H.L. and X.G.; methodology, H.L.; software, H.L.; validation, H.L., Y.J. and X.G.; formal analysis, H.L. and H.Z.; investigation, H.L., Z.W., Y.L., H.X., Y.J. and H.Q.; resources, H.Q. and X.G.; data curation, Z.W., Y.L. and H.X.; writing—original draft preparation, H.L.; writing—review & editing, H.L., X.G. and Y.J.; visualization, H.L.; supervision, X.G. and H.Q.; project administration, X.G. and H.Q.; funding acquisition, Y.J. and H.Q. All authors have read and agreed to the published version of the manuscript.

Funding: This research was funded by the National Natural Science Foundation of China (32071976, 31901471), the Science and Technology Program in Liaoning Province of China (2021-BS-144, 2021JH2/10200013) and the China Postdoctoral Science Foundation (2019M661130).

Data Availability Statement: Our study did not report to any data.

Conflicts of Interest: The authors declare no conflict of interest. The funders had no role in the design of the study; in the collection, analyses, or interpretation of data; in the writing of the manuscript, or in the decision to publish the results.

References

1. Zhang, W.; Li, S.; Xu, Y.; Wang, J. Residue incorporation enhances the effect of subsoiling on soil structure and increases SOC accumulation. *J. Soils Sediments* **2020**, *20*, 3537–3547. [[CrossRef](#)]
2. Xu, X.; Schaeffer, S.; Sun, Z.; Wang, J.K. Carbon stabilization in aggregate fractions responds to straw input levels under varied soil fertility levels. *Soil Tillage Res.* **2020**, *199*, 104593. [[CrossRef](#)]
3. Li, L.J.; Burger, M.; Du, S.L.; Han, X.Z. Change in soil organic carbon between 1981 and 2011 in croplands of Heilongjiang Province, Northeast China. *J. Sci. Food Agric.* **2016**, *96*, 1275–1283. [[CrossRef](#)] [[PubMed](#)]
4. Xie, H.T.; Li, J.W.; Zhu, P.; Peng, C.; Wang, J.K.; He, H.B.; Zhang, X.D. Long-term manure amendments enhance neutral sugar accumulation in bulk soil and particulate organic matter in a Mollisol. *Soil Biol. Biochem.* **2014**, *78*, 45–53. [[CrossRef](#)]
5. Zhang, S.; Chen, X.; Jia, S.; Liang, A.; Zhang, X.; Yang, X.; Wei, S.; Sun, B.; Huang, D.; Zhou, G. The potential mechanism of long-term conservation tillage effects on maize yield in the black soil of Northeast China. *Soil Tillage Res.* **2015**, *154*, 84–90. [[CrossRef](#)]
6. Wang, S.; Zhao, Y.; Wang, J.; Gao, J.; Zhu, P.; Cui, X.; Lu, C. Estimation of soil organic carbon losses and counter approaches from organic materials in black soils of northeastern China. *J. Soils Sediments* **2019**, *20*, 1241–1252. [[CrossRef](#)]
7. Lal, R. Challenges and opportunities in soil organic matter research. *Eur. J. Soil Sci.* **2009**, *60*, 158–169. [[CrossRef](#)]
8. Wang, H.; Wang, S.; Zhang, Y.; Wang, X.; Wang, R.; Li, J. Tillage system change affects soil organic carbon storage and benefits land restoration on loess soil in North China. *Land Degrad. Dev.* **2018**, *29*, 2880–2887. [[CrossRef](#)]
9. Xia, L.; Lam, S.K.; Wolf, B.; Kiese, R.; Chen, D.; Butterbach-Bahl, K. Trade-offs between soil carbon sequestration and reactive nitrogen losses under straw return in global agroecosystems. *Glob. Change Biol.* **2018**, *24*, 5919–5932. [[CrossRef](#)]
10. Makarov, M.I.; Mulyukova, O.S.; Malysheva, T.I.; Menyailo, O.V. Influence of drying of the samples on the transformation of nitrogen and carbon compounds in mountain-meadow alpine soils. *Eurasian Soil Sci.* **2013**, *46*, 778–787. [[CrossRef](#)]
11. MacCarthy, P. The principles of humic substances. *Soil Sci.* **2001**, *166*, 738–751. [[CrossRef](#)]
12. Plaza, I.; Ontiveros-Ortega, A.; Calero, J.; Aranda, V. Implication of zeta potential and surface free energy in the description of agricultural soil quality: Effect of different cations and humic acids on degraded soils. *Soil Tillage Res.* **2015**, *146*, 148–158. [[CrossRef](#)]
13. Zhang, M.; Cheng, G.; Feng, H.; Sun, B.; Zhao, Y.; Chen, H.; Chen, J.; Dyck, M.; Wang, X.; Zhang, J.; et al. Effects of straw and biochar amendments on aggregate stability, soil organic carbon, and enzyme activities in the Loess Plateau, China. *Environ. Sci. Pollut. Res. Int.* **2017**, *24*, 10108–10120. [[CrossRef](#)] [[PubMed](#)]
14. Duval, M.E.; Galantini, J.A.; Martínez, J.M.; Limbozzi, F. Labile soil organic carbon for assessing soil quality: Influence of management practices and edaphic conditions. *Catena* **2018**, *171*, 316–326. [[CrossRef](#)]
15. Jastrow, J.D. Soil aggregate formation and the accrual of particulate and mineral-associated organic matter. *Soil Biol. Biochem.* **1996**, *28*, 665–676. [[CrossRef](#)]
16. Sarker, J.R.; Singh, B.P.; Cowie, A.L.; Fang, Y.Y.; Collins, D.; Dougherty, W.J.; Singh, B.K. Carbon and nutrient mineralisation dynamics in aggregate-size classes from different tillage systems after input of canola and wheat residues. *Soil Biol. Biochem.* **2018**, *116*, 22–38. [[CrossRef](#)]
17. Brar, B.S.; Singh, K.; Dheri, G.S. Carbon sequestration and soil carbon pools in a rice-wheat cropping system: Effect of long-term use of inorganic fertilizers and organic manure. *Soil Tillage Res.* **2013**, *128*, 30–36. [[CrossRef](#)]
18. Lugato, E.; Simonetti, G.; Morari, F.; Nardi, S.; Berti, A.; Giardini, L. Distribution of organic and humic carbon in wet-sieved aggregates of different soils under long-term fertilization experiment. *Geoderma* **2010**, *157*, 80–85. [[CrossRef](#)]
19. Duval, M.E.; Galantini, J.A.; Iglesias, J.O.; Canelo, S.; Martínez, J.M.; Wall, L. Analysis of organic fractions as indicators of soil quality under natural and cultivated systems. *Soil Tillage Res.* **2013**, *131*, 11–19. [[CrossRef](#)]
20. Somasundaram, J.; Reeves, S.; Wang, W.J.; Heenan, M.; Dalal, R. Impact of 47 years of no tillage and stubble retention on soil aggregation and carbon distribution in a Vertisol. *Land Degrad. Dev.* **2017**, *28*, 1589–1602. [[CrossRef](#)]
21. Blanco-Canqui, H.; Ruis, S.J. No-tillage and soil physical environment. *Geoderma* **2018**, *326*, 164–200. [[CrossRef](#)]
22. Zhang, Y.; Li, X.; Gregorich, E.G.; McLaughlin, N.B.; Zhang, X.; Guo, Y.; Liang, A.; Fan, R.; Sun, B. No-tillage with continuous maize cropping enhances soil aggregation and organic carbon storage in Northeast China. *Geoderma* **2018**, *330*, 204–211. [[CrossRef](#)]
23. Wang, X.; Qi, J.Y.; Zhang, X.Z.; Li, S.S.; Virk, A.L.; Zhao, X.; Xiao, X.P.; Zhang, H.L. Effects of tillage and residue management on soil aggregates and associated carbon storage in a double paddy cropping system. *Soil Tillage Res.* **2019**, *194*, 104339. [[CrossRef](#)]
24. Alidad, K.; Mehdi, H.; Sadegh, A.; Hassan, R.; Sanaz, B. Organic resource management: Impacts on soil aggregate stability and other soil physico-chemical properties. *Agric. Ecosyst. Environ.* **2012**, *148*, 22–28. [[CrossRef](#)]
25. Huang, R.; Tian, D.; Liu, J.; Lv, S.; He, X.; Gao, M. Responses of soil carbon pool and soil aggregates associated organic carbon to straw and straw-derived biochar addition in a dryland cropping mesocosm system. *Agric. Ecosyst. Environ.* **2018**, *265*, 576–586. [[CrossRef](#)]
26. Dou, S.; Shan, J.; Song, X.; Cao, R.; Wu, M.; Li, C.; Guan, S. Are humic substances soil microbial residues or unique synthesized compound? *Pedosphere* **2020**, *30*, 159–167. [[CrossRef](#)]
27. Dheri, G.S.; Lal, R.; Moonilall, N.I. Soil carbon stocks and water stable aggregates under annual and perennial biofuel crops in central Ohio. *Agric. Ecosyst. Environ.* **2022**, *324*, 107715. [[CrossRef](#)]

28. Zhang, J.; Wei, Y.; Liu, J.; Yuan, J.; Liang, Y.; Ren, J.; Cai, H. Effects of maize straw and its biochar application on organic and humic carbon in water-stable aggregates of a Mollisol in Northeast China: A five-year field experiment. *Soil Tillage Res.* **2019**, *190*, 1–9. [[CrossRef](#)]
29. Peixoto, D.S.; da Silva, L.D.C.M.; Melo, L.; Azevedo, R.P.; Silva, B.M. Occasional tillage in no-tillage systems: A global meta-analysis. *Sci. Total Environ.* **2020**, *745*, 140887. [[CrossRef](#)]
30. Staff, S.S. *Keys to Soil Taxonomy*, 11th ed.; United States Department of Agriculture, Natural Resources Conservation Service: Washington, DC, USA, 2010.
31. Głab, T.; Kulig, B. Effect of mulch and tillage system on soil porosity under wheat (*Triticum aestivum*). *Soil Tillage Res.* **2008**, *99*, 169–178. [[CrossRef](#)]
32. Dorich, R.A.; Nelson, D.W. Evaluation of Manual Cadmium Reduction Methods for Determination of Nitrate in Potassium Chloride Extracts of Soils. *Soil Sci. Soc. Am. J.* **1984**, *48*, 72. [[CrossRef](#)]
33. Hedley, M.J.; Stewart, J.W.B. Method to measure microbial phosphate in soils. *Soil Biol. Biochem.* **1982**, *14*, 377–385. [[CrossRef](#)]
34. Warncke, D.; Brown, J.R. Potassium and Other Basic Cations. In *Recommended Chemical Soil Test Procedures for the North Central Region*; Missouri Agricultural Experiment Station SB 1001: Columbia, MO, USA, 2011; Volume 1998, p. 31.
35. Kemper, W.D.; Rosenau, R.C. Aggregate Stability and Size Distribution. In *Methods of Soil Analysis. Part 1. Physical and Mineralogical Methods-Agronomy Monograph 9*; American Society of Agronomy: Madison, WI, USA, 1986; pp. 425–442.
36. Rivero, C.; Chirenje, T.; Ma, L.Q.; Martinez, G. Influence of compost on soil organic matter quality under tropical conditions. *Geoderma* **2004**, *123*, 355–361. [[CrossRef](#)]
37. Elliott, E.T. Aggregate Structure and Carbon, Nitrogen, and Phosphorus in Native and Cultivated Soils. *Soil Sci. Soc. Am. J.* **1986**, *50*, 627. [[CrossRef](#)]
38. Jastrow, J.D.; Amonette, J.E.; Bailey, V.L. Mechanisms controlling soil carbon turnover and their potential application for enhancing carbon sequestration. *Clim. Change* **2006**, *80*, 5–23. [[CrossRef](#)]
39. Qi, J.Y.; Jing, Z.H.; He, C.; Liu, Q.Y.; Wang, X.; Kan, X.-R.; Zhao, X.; Xiao, X.-P.; Zhang, H.-L. Effects of tillage management on soil carbon decomposition and its relationship with soil chemistry properties in rice paddy fields. *J. Environ. Manag.* **2020**, *279*, 111595. [[CrossRef](#)]
40. Piccolo, A.; Pietramellara, G.; Mbagwu, J.S.C. Use of humic substances as soil conditioners to increase aggregate stability. *Geoderma* **1997**, *75*, 267–277. [[CrossRef](#)]
41. Bronick, C.J.; Lal, R. Soil structure and management: A review. *Geoderma* **2005**, *124*, 3–22. [[CrossRef](#)]
42. Ashagrie, Y.; Zech, W.; Guggenberger, G.; Mamo, T. Soil aggregation, and total and particulate organic matter following conversion of native forests to continuous cultivation in Ethiopia. *Soil Tillage Res.* **2007**, *94*, 101–108. [[CrossRef](#)]
43. Fernández, R.; Quiroga, A.; Zorati, C.; Noellemeyer, E. Carbon contents and re-spiration rates of aggregate size fractions under no-till and conventional tillage. *Soil Tillage Res.* **2010**, *109*, 103–109. [[CrossRef](#)]
44. Schmidt, E.S.; Villamil, M.B.; Amiotti, N.M. Soil quality under conservation practices on farm operations of the southern semiarid pampas region of Argentina. *Soil Tillage Res.* **2018**, *176*, 85–94. [[CrossRef](#)]
45. Six, J.; Elliott, E.T.; Paustian, K. Soil macroaggregate turnover and micro-aggregate formation: A mechanism for C sequestration under no-tillage agriculture. *Soil Biol. Biochem.* **2000**, *32*, 2099–2103. [[CrossRef](#)]
46. Blanco-Canqui, H.; Stone, L.R.; Schlegel, A.J.; Lyon, D.J.; Vigil, M.F.; Mikha, M.M.; Stahlman, P.W.; Rice, C.W. No-till induced increase in organic carbon reduces maximum bulk density of soils. *Soil Sci. Soc. Am. J.* **2009**, *73*, 1871–1879. [[CrossRef](#)]
47. Six, J.; Paustian, K.; Elliott, E.T.; Combrink, C. Soil structure and organic matter I. Distribution of aggregate-size classes and aggregate-associated carbon. *Soil Sci. Soc. Am. J.* **2000**, *64*, 681–689. [[CrossRef](#)]
48. Dou, S.; Zhang, J.J.; Li, K. Effect of organic matter applications on ¹³C-NMR spectra of humic acids of soil. *Eur. J. Soil Sci.* **2008**, *59*, 532–539. [[CrossRef](#)]
49. Lutzow, M.V.; Kogel-Knabner, I.; Ekschmitt, K.; Matzner, E.; Guggenberger, G.; Marschner, B.; Flessa, H. Stabilization of organic matter in temperate soils: Mechanisms and their relevance under different soil conditions—a review. *Eur. J. Soil Sci.* **2006**, *57*, 426–445. [[CrossRef](#)]
50. Ingelmo, F.; Molina, M.J.; Soriano, M.D.; Gallardo, A.; Lapeña, L. Influence of organic matter transformations on the bioavailability of heavy metals in a sludge based compost. *J. Environ. Manag.* **2012**, *95*, 104–109. [[CrossRef](#)]
51. Senesi, N. Humic Substances as Natural Nanoparticles Ubiquitous in the Environment. In *Molecular Environmental Soil Science at the Interfaces in the Earth's Critical Zone*; Xu, J.M., Huang, P.M., Eds.; Springer: Berlin/Heidelberg, Germany, 2010; pp. 249–250.
52. Calza, P.; Vione, D.; Minero, C. The role of humic and fulvic acids in the phototransformation of phenolic compounds in seawater. *Sci. Total Environ.* **2014**, *493*, 411–418. [[CrossRef](#)]